SEMARAK ILMU PUBLISHING

Journal of Advanced Research in Applied Sciences and Engineering Technology

Journal homepage:
https://semarakilmu.com.my/journals/index.php/applied_sciences_eng_tech/index
ISSN: 2462-1943

Optimization of Synthesizing Conditions for MXene (Ti_3C_2) Photocatalyst: Effect of LiF:Ti_3AlC_2 Mass Ratio

Nabilah Saafie[1], Suriati Sufian[2,*], Farah Amelia Shahirah Roslan[1], Muhamad Irfan Khan[1]

[1] Chemical Engineering Department, Universiti Teknologi PETRONAS, Seri Iskandar 32610, Perak, Malaysia
[2] Center of Innovative Nanostructures and Nanodevices (COINN), Universiti Teknologi PETRONAS, Seri Iskandar 32610, Perak, Malaysia

ARTICLE INFO

Article history:
Received 12 July 2023
Received in revised form 1 August 2023
Accepted 4 March 2024
Available online 25 June 2024

Keywords:
MXene; photocatalytic degradation; methylene blue

ABSTRACT

The analysis of the proposed work, specifically the development of the MXene photocatalyst, will be described in this chapter. The results of the analysis are useful for comparing the pristine precursor and etched structures of the MXene photocatalyst. A minimally intensive layer delamination (MILD) method will be used to create the MXene photocatalyst which uses lower fluorine content solution (HCl-LiF) creating a safer and easier method. The synthesis parameters for the development of highly efficient MXene photocatalysts, such as LiF:Ti_3AlC_2 mass ratio will be optimized. FTIR, XRD, SAP, FESEM and DR UV-Vis analysis will be used to characterize the as-developed MXene photocatalyst and its precursor, Ti_3AlC_2. The hypothesis of this study is etching treatment will increase the hydrophilicity and active functional group such as oxygen (O), fluorine (F) and hydroxyl (-OH) on MXene surfaces. The performance of photocatalytic degradation will be tested with an initial dye concentration of 30 ppm, solution pH at pH7 at room temperature (±27˚C). Each photocatalytic degradation study was performed in 50 ml of methylene blue solution with 0.1 g photocatalyst. All developed MXenes will undergo photocatalytic degradation performance to identify the optimized synthesizing conditions. The highest MXene photodegradation performance was found to reach 90% removal within 180 min.

1. Introduction

The growth in industrial and agricultural activities in recent years has assigned major responsibility for the continuous discharge of toxic organic contaminants into water bodies without treatment. As a result of the toxic chemicals and gases emitted by industrial and agricultural activities, this growth has been shown to contribute to the rise in water pollution over the century [1]. According to the Natural Resources Defense Council (NRDC), industrial wastewater pollution affects about 1 billion people worldwide each year, with low-income populations being disproportionately affected because their residences are often closer to polluting companies. Furthermore, excessive pollutants such as heavy metals, dyes, and antibiotics were dumped into the water body without sufficient wastewater treatment [2,3].

* *Corresponding author.*
E-mail address: suriati@utp.edu.my

https://doi.org/10.37934/araset.47.2.183192

Photocatalysis has been shown to be a cheap, easy, efficient, and rapid treatment procedure for complete dye removal using suitable photocatalysts and a light source [4,5]. In addition, due to the mild conditions and environmentally friendly characteristics, photocatalytic technology has been diffusely investigated by combining the solar energy with photocatalysts in environmental remediation and energy field, such as the degradation of pollutants in water or air, hydrogen (H_2) production, carbon dioxide (CO_2) reduction and nitrogen (N_2) fixation [6]. Besides, photocatalysis can generate many reactive species that can effectively destroy and degrade organic contaminants [7]. Principally, photocatalysis steps take account of transferring the liquid phase reactants to the catalyst surface, adsorbing the reactants to the catalyst surface, reacting in the absorbing phase, desorbing the final product, and finally removing the final product in the liquid phase.

MXene has captivated researchers' interest as a promising environmental photocatalyst, particularly for treating wastewater containing dyes [1]. Mxene materials have gotten a lot of attention because of their wide range of unique structure characteristics, high specific surface area and outstanding physicochemical properties [8]. The MXene compound has a higher reflectivity in the ultraviolet (UV) light correspond to the visible light absorptions with a reported wavelength range of 300 to 500 nm, which is important for photocatalytic reactions with energy gaps of 0.25 to 2.0 eV [9]. MXene also has a hydrophilic character, which is combined with hydrophicity and an active functional group on its surface, which extracts the adsorptive nature to deal with ionic/molecular species for environmental remediation [10].

According to that, a preliminary synthesis of MXene photocatalyst development were evaluated in this chapter before using it as co-catalyst in heterojunction composite for an optimal manner. The etching procedure resulted in the improvement of hydrophilic compounds due to the functionalization of MXene. However, depending on the precursor mass, etching concentrations, and circumstances, the approaches may reduce photodegradation performance [11]. These also affect the presence of functional groups on MXene surface. Therefore, this present research objectives are to compare the pristine and composite structures of MXene photocatalyst and evaluate their photocatalytic degradation. A minimally intensive layer delamination (MILD) method was chosen which uses lower fluorine content solution (HCl-LiF) creates a safer and easier method.

2. Methodology

2.1 Synthesizing the MXene Photocatalyst

The MXene photocatalyst was developed using the minimally intensive layer delamination (MILD) method [11]. In a typical procedure, 3.2 g LiF was gradually added to 10 ml of 9 M HCl and stirred continuously for 5 minutes. Then, 2.0 g of Ti_3AlC_2 powder was gradually added, and the etching process was allowed to run for 24 hours at room temperature. The as synthesized resultants were determined as MXene-1.6 which meant the mass ratio of LiF:Ti_3AlC_2. The typical method etching process was repeated for MXene-1.0 and MXene-2.0. The MXene powder was then separated and cleaned with deionized water using a centrifuge process at 3500 rpm for 5 minutes per cycle. The washing procedure continued until the pH of the supernatant was about neutral. The MXene powder particles were then rewashed with 500 ml deionized water by vacuum assisted filtering before being dried at 120°C for 24 hours.

2.2 Characterization of MXene Photocatalyst

The surface functional groups for MXene photocatalysts were characterized using FTIR spectroscopy (Perkin Elmer Spectrum One, FTIR-Frontier, U.S.A) using KBr pellet method. Their FTIR

spectroscopy results were scanned and recorded in the range of 400 to 4000 cm^{-1}. A Powder X-ray Diffractometer was used to analyse the materials using X-ray Diffraction Analysis (XRD) (PANalytical, X'pert Powder, Netherland) in the 2θ angle ranging from 10˚ to 80˚ incremented by 0.02˚ step size. Field Emission Scanning Electron Microscope (FESEM) (Carl Zeiss, Supra 55 VP Scanning Electron Microscope, U.S.A) was used to examine the structures and surface morphologies of MXene. Based on the nitrogen adsorption-desorption method, the specific surface area, pore volume, and pore size distribution of surface area analyzer and Porosity analysis (SAP) (Micromeritics Tristar II, Surface Area and Porosity, U.S.A) were obtained. The absorption spectrum was estimated using a DRS UV-Vis, UV 3150 NIR (Shimadzu, Japan) spectrophotometer constructed with an integrated sphere.

2.3 Photocatalytic Degradation Analysis

In a photoreactor with a magnetic stirrer, studies on photocatalytic degradation were conducted. An aluminium foil cover will be placed over a 100 mL beaker to prevent radiation leakage. The suspension was positioned 15 cm distant from the beaker to increase visible light irradiation. At pH 7 and 30°C, testing for the photocatalytic degradation of synthetic Methylene Blue (MB) will be conducted. MXene powder (100 mg) was mixed in 50 mL of 30 ppm MB aqueous solution. The suspension was stirred in the dark for 30 minutes to ensure an equilibrium adsorption-desorption state [12]. Following that, cooling fans were used to keep the solution temperature stable, and a 500 W Halogen lamp was used to provide continuous stirring (150 rpm). A sample of 0.1 ml from the solution will be taken using a micropipette every 30 minutes, and it will be examined using a UV-Vis spectrophotometer (UV-1800, Shimadzu).

2.4 Methylene Blue Degradation Analysis

Powdered MB was dissolved in deionized water to create synthetic wastewater. The precise peak of MB's absorption at 664 nm was chosen as the typical peak for concentrations. The following equation will be used to estimate the MB degrading efficiency (%):

$$MB\ degradation\ efficiency = \frac{C_0 - C_t}{C_0} \times 100 \quad (1)$$

where C_0 and C_t (mg/L) represents to initial and at certain time concentrations of MB, respectively.

3. Results

3.1 Characterization of MXene Photocatalyst

As shown in Figure 1, FTIR spectroscopy was utilised to further examine the functional group compositions of Ti_3AlC_2, MXene-1.0, MXene-1.6, and MXene-2.0. The surface chemistry bands displayed by the FTIR spectra of O−H stretching and bending at 3431 and 1628 cm^{-1}, respectively showed higher transmittance changed for MXenes compared to Ti_3AlC_2 [13]. This indicates that higher oxygen terminated functional groups were introduced due to the etching process. Since the fluoride salts were used in the etching process, the enhancement of peak intensity of C−F band at 1400 cm^{-1} was noticed [14]. Presence of new functional group was identified at 571 cm^{-1} attributed to Ti-O bond vibration, originates from the surface adsorption of −OH [15]. Methylene blue preferentially degrades when an oxygen-containing surface group is present, which is a desired attractive site for cationic dyes [16].

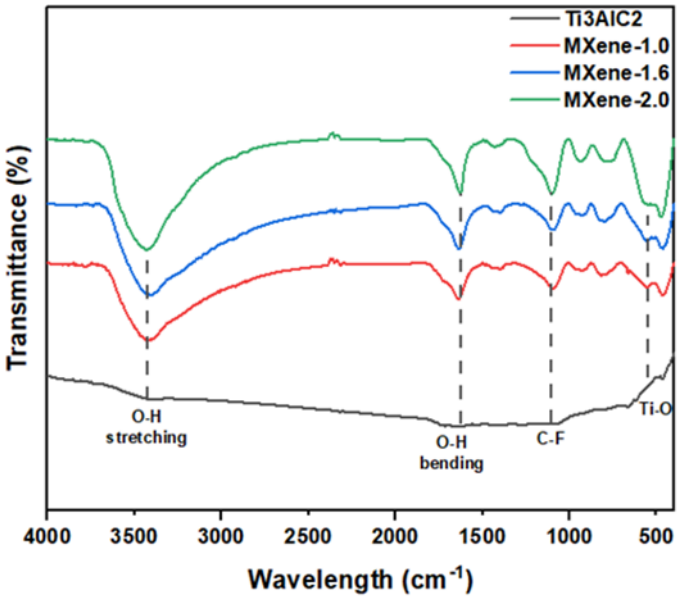

Fig. 1. FTIR Spectra

Ti_3AlC_2, MXene-1.0, MXene-1.6, and MXene-2.0's phase composition was examined using XRD analysis. As shown in Figure 2, all exhibited almost the same XRD patterns, except for some new peaks located at 2θ = 13.1°, 45.2° and 65.5° which denoted as Ti_3C_2 [17]. This proved the transformation of Ti_3AlC_2 to Ti_3C_2 causing by LiF etching. The Ti_3C_2OH's distinctive peaks were seen at 2θ = 19.3°, 48.6°, 56.6°, 60.3° and 71.8° which also confirmed the successful fabrication of MXene. However, the intensity peaks of Ti_3AlC_2 were remained and reduced after treatment due to the incomplete etching using LiF/HCl agents [11]. Table 1 shows the compound composition to assess the score percentage of each phase. After the optimization of synthesizing conditions process MXene-1.6 has the highest Ti_3C_2 compound score, 69% compared to MXene-1.0 and MXene 2.0.

Table 1
Compound composition score by XRD

Photocatalyst	Percentage (%)		
	Ti_3AlC_2	Ti_3C_2	Ti_3C_2OH
Ti_3AlC_2	100	NA	NA
MXene-1.0	62	31	7
MXene-1.6	26	69	5
MXene-2.0	31	64	5

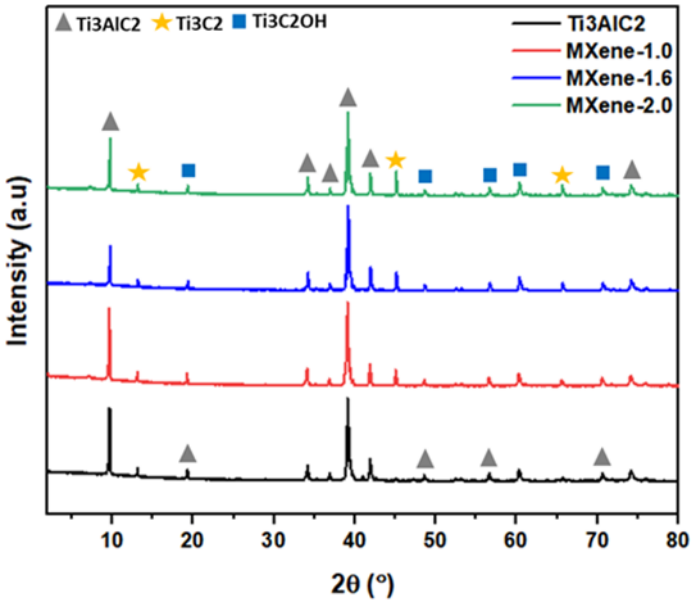

Fig. 2. XRD Patterns

The DR-UV-Vis characteristics of the Ti_3AlC_2, MXene-1.0, MXene-1.6, and MXene-2.0 samples were shown in Figure 3(a). It is strongly supported that the titanium carbide photocatalyst was a visible-light-driven photocatalyst based on the band gap absorption edge of the samples' resilient absorption capacity in the visible light regime [17]. The band gap energy for the titanium carbide photocatalyst is depicted in Figure 3(b) by extrapolating from the curve of (αhv)2 versus (hv). Ti_3AlC_2, MXene-1.0, MXene-1.6, and MXene-2.0 had computed band gaps of 1.37, 1.25, 1.23, and 1.27 eV, respectively. The measured band gap energy agreed with previous findings with band gap energies ranging from 0.25 to 2.0 eV [18].

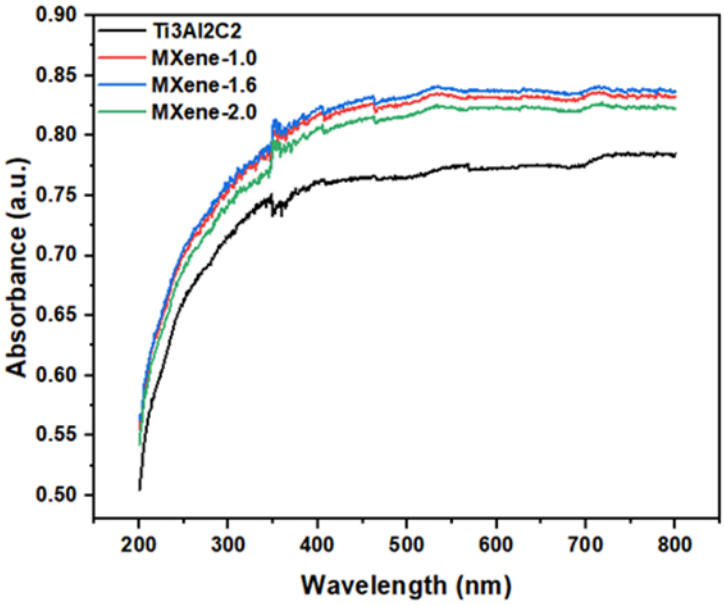

(a)

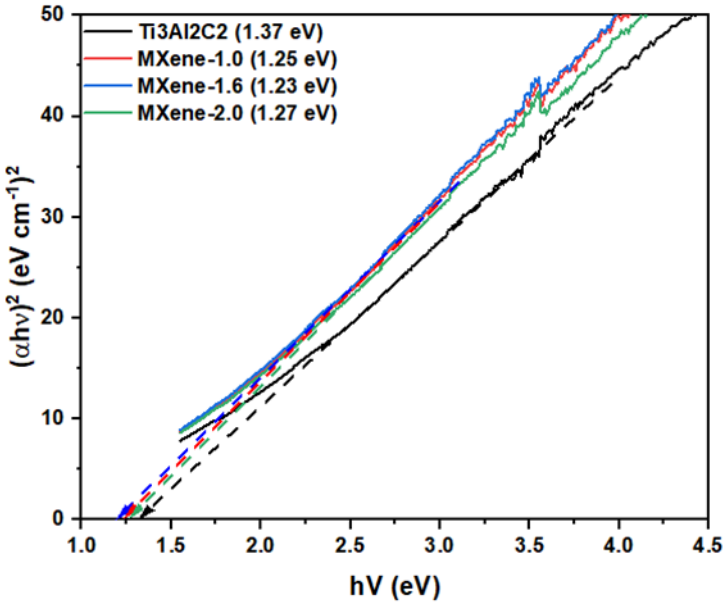

(b)

Fig. 3. (a) Absorbance Spectra, (b) Tauc Plot

It is anticipated that photogenerated holes and photoexcited electrons will be easier to move and migrate due to the narrow band gap energy's reduced photon energy need, which is in line with the capacity to absorb visible light. The efficiency of photocatalytic degradation will rise as a result. Additionally, in the heterostructure concept, highly conductive MXenes with known low bandgap energies would make it easier to collect electrons produced by other semiconductors [19]. The migration of generated electrons was favourable to increase separation efficiency of charge carriers and inhibit the electron-hole recombination.

The morphological structures of Ti_3AlC_2 and MXene-1.6 are presented in Figure 4(a), Figure 4(c) and Figure 4(b), Figure 4(d), respectively. The FESEM images showed that the MXene-1.6 yielded stacked carbon layer with opening lamellas and pores compare to MAX phase, Ti_3AlC_2 appeared as large block morphology. The basic basis for the production of the layered structure, where structural holes can be clearly seen, is the chemical exfoliation of the A group element, Al, during the etching operation [20]. As shown in Table 2, the elemental composition of Al element was plunged from 14.92 wt% in Ti_3AlC_2 to 0.33 wt% in MXene-1.6. This data proved that Al layers were exfoliated, and layer distances expanded. Therefore, Ti_3C_2Tx owing higher surface area which increases the exposed surface functional groups thus expected to improve the photodegradation activity. Furthermore, O element was also increased after etching treatment from 9.78 wt% in Ti_3AlC_2 to 13.01 wt% in MXene-1.6.

Both Ti_3AlC_2 and MXene-1.6 shows type IV isotherm showing H3 type hysteresis loop in Figure 5 which indicated parallel plate shaped pores [21]. As shown in the image, MXene-1.6 has more volume adsorbed at the isotherm 'knee' than Ti_3AlC_2, indicating that its surface area has increased. This could be explained by the increasing of layer spacing during etching treatment where Al was removed. Table 2 lists the texture metrics, including the Brunauer Emmet Teller (BET) surface area, total pore volume, and average pore diameter. The result confirmed that the MXene-1.6 had higher surface area 3.11 m^2/g compared to the precursor Ti_3AlC_2, 1.68 m^2/g. The results obtained agreed with previous work carried out by Qu *et al.,* [15] which reported 2.17 m^2/g surface area after HF-forming etchants treatment.

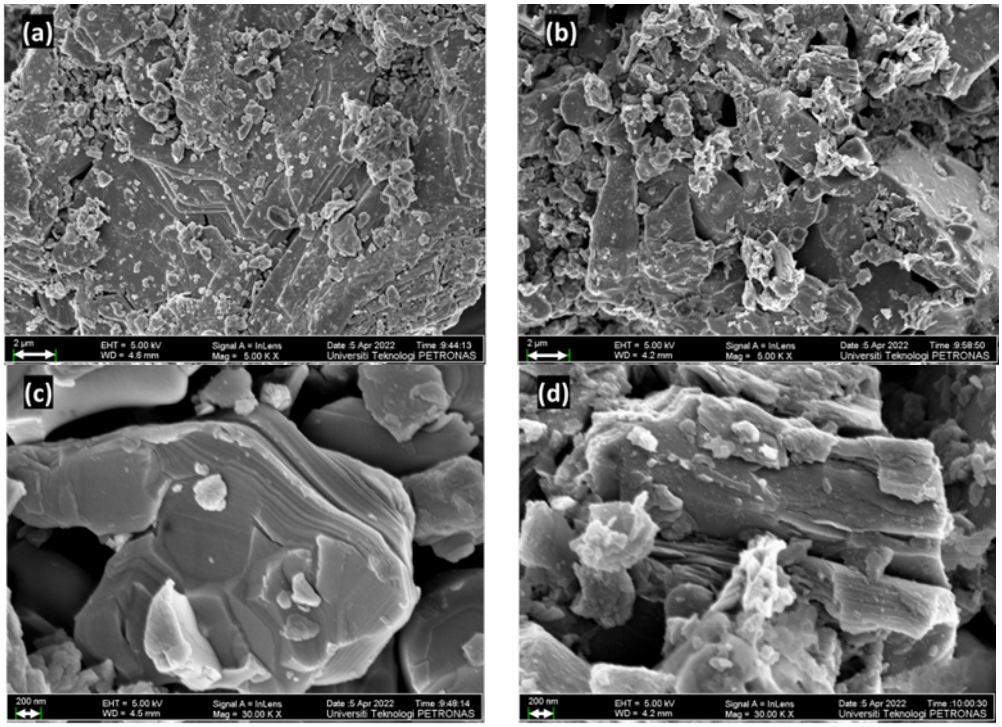

Fig. 4. FESEM micrographs of (a, c) Ti_3AlC_2 (b, d) MXene-1.6 at 5.00 K and 30.00 K magnification, respectively

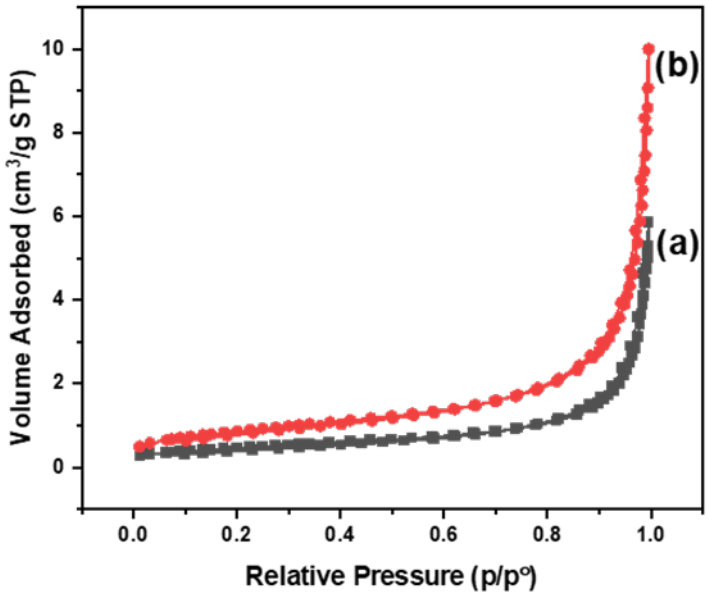

Fig. 5. N2 adsorption-desorption isotherm of (a) Ti_3AlC_2 and (b) MXene-1.6

Table 2
SAP analysis of the Ti_3AlC_2 and MXene-1.6

Photocatalyst	Surface Area (m^2/g)	Pore Volume (cm^3/g)	Pore size (nm)
Ti_3AlC_2	1.68	0.01	18.50
MXene-1.6	3.11	0.01	17.10

3.1 Photocatalytic Degradation Performance

In a batch setup using MB solutions, the effectiveness of Ti_3AlC_2, MXene-1.0, MXene-1.6, and MXene-2.0 was assessed. The results shown in Figure 6 that a massive difference between the samples in terms of the amount of time needed to get the dye down to a safe level. The MXene-1.6 shows the highest adsorption rate with 90% of MB being removed within 180 minutes. Meanwhile, MXene-1.0 and MXene-2.0 only managed to removed MB ~45% and ~60%, respectively within the same timeframe. This outcome was agreed with the elemental composition by EDX spot where MXene-1.6 give the higher oxygen terminated functional groups were introduced due to the etching process. MXene 1.6 also has a hydrophilic nature that is combined with hydrophilicity and active functional groups like oxygen (-O), fluorine (F), and hydroxyl (-OH) on its surface, which extracts the adsorptive nature to deal with ionic/molecular species for environmental resolution [21].

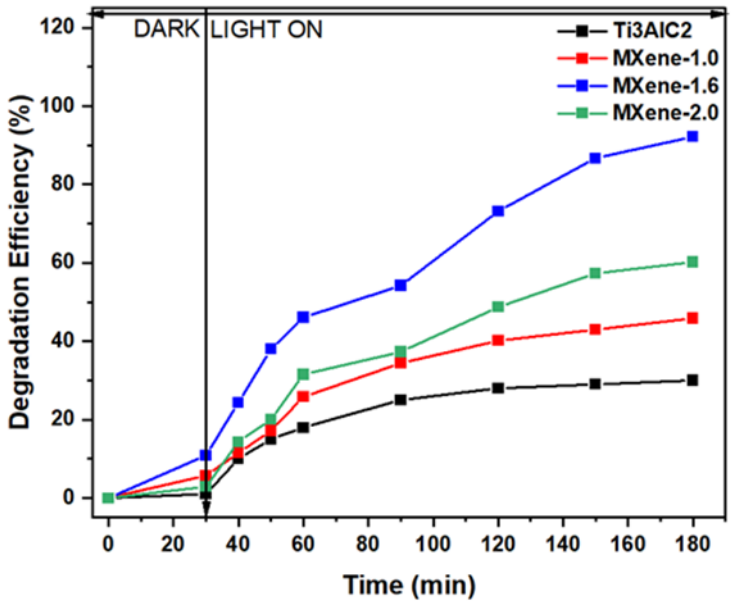

Fig. 6. Decolorization of MB (30 ppm)

4. Conclusions

In this work, MXene-1.6 showed the best LiF:Ti_3AlC_2 mass ratio to synthesize MXene photocatalyst. It offers an adequate number of significant functional groups to connect to the surface of MXene during the etching process. The XRD data revealed that the transformation of Ti_3AlC_2 to Ti_3C_2 causing by LiF etching was successful and MXene-1.6 has the highest Ti_3C_2 compound score, 69% compared to MXene-1.0 and MXene 2.0. The greater BET surface area of MXene 1.6 (3.11 m^2/g) compared to the precursor Ti_3AlC_2 (1.68 m^2/g) was further validated by a FESEM micrograph. The adsorption analysis indicates that MXene-1.6 has the maximum degradation rate, removing 90% of MB in about 180 minutes. Therefore, a minimally intensive layer delamination (MILD) method successfully created the MXene photocatalyst using lower fluorine content solution (HCl-LiF) with 1.6 of LiF:Ti_3AlC_2 mass ratio.

Acknowledgement
This research was funded by a grant from Ministry of Higher Education of Malaysia (FRGS/1/2020/TK0/UTP/02/22) and Yayasan Universiti Teknologi PETRONAS, YUTP (015LC0 357).

References

[1] Jun, Byung-Moon, Sewoon Kim, Hojung Rho, Chang Min Park, and Yeomin Yoon. "Ultrasound-assisted Ti_3C_2Tx MXene adsorption of dyes: Removal performance and mechanism analyses via dynamic light scattering." *Chemosphere* 254 (2020): 126827. https://doi.org/10.1016/j.chemosphere.2020.126827

[2] Rethinasabapathy, Muruganantham, Gokul Bhaskaran, Bumjun Park, Jin-Yong Shin, Woo-Sik Kim, Jungho Ryu, and Yun Suk Huh. "Iron oxide (Fe_3O_4)-laden titanium carbide (Ti_3C_2Tx) MXene stacks for the efficient sequestration of cationic dyes from aqueous solution." *Chemosphere* 286 (2022): 131679. https://doi.org/10.1016/j.chemosphere.2021.131679

[3] Kiew, Peck Loo, Nur Ainaa Mohd Fauzi, Shania Aufaa Firdiani, Man Kee Lam, Lian See Tan, and Wei Ming Yeoh. "Iron oxide nanoparticles derived from Chlorella vulgaris extract: Characterization and crystal violet photodegradation studies." *Progress in Energy and Environment* 24 (2023): 1-10. https://doi.org/10.37934/progee.24.1.110

[4] Isa, Eleen Dayana Mohamed, Kamyar Shameli, Nurfatehah Wahyuny Che Jusoh, Siti Nur Amalina Mohamad Sukri, and Nur'Afini Ismail. "Photocatalytic Degradation with Green Synthesized Metal Oxide Nanoparticles-A Mini Review." *Journal of Research in Nanoscience and Nanotechnology* 2, no. 1 (2021): 70-81. https://doi.org/10.37934/jrnn.2.1.7081

[5] Yu, Mingchuan, Huanjing Liang, Ruonan Zhan, Lei Xu, and Junfeng Niu. "Sm-doped g-C_3N_4/Ti_3C_2 MXene heterojunction for visible-light photocatalytic degradation of ciprofloxacin." *Chinese Chemical Letters* 32, no. 7 (2021): 2155-2158. https://doi.org/10.1016/j.cclet.2020.11.069

[6] Liu, Wenzhu, Mingxuan Sun, Zhipeng Ding, Bowen Gao, and Wen Ding. "Ti_3C_2 MXene embellished g-C_3N_4 nanosheets for improving photocatalytic redox capacity." *Journal of Alloys and Compounds* 877 (2021): 160223. https://doi.org/10.1016/j.jallcom.2021.160223

[7] Zhou, Yufei, Mingchuan Yu, Ruonan Zhan, Xiaojing Wang, Guowen Peng, and Junfeng Niu. "Ti_3C_2 MXene-induced interface electron separation in g-C_3N_4/ Ti_3C_2 MXene/$MoSe_2$ Z-scheme heterojunction for enhancing visible light-irradiated enoxacin degradation." *Separation and Purification Technology* 275 (2021): 119194. https://doi.org/10.1016/j.seppur.2021.119194

[8] Cui, Yi, Dongao Zhang, Kelin Shen, Siqing Nie, Meiying Liu, Hongye Huang, Fengjie Deng, Naigen Zhou, Xiaoyong Zhang, and Yen Wei. "Biomimetic anchoring of Fe_3O_4 onto Ti_3C_2 MXene for highly efficient removal of organic dyes by Fenton reaction." *Journal of Environmental Chemical Engineering* 8, no. 5 (2020): 104369. https://doi.org/10.1016/j.jece.2020.104369

[9] Kannan, Karthik, Kishor Kumar Sadasivuni, Aboubakr M. Abdullah, and Bijandra Kumar. "Current trends in MXene-based nanomaterials for energy storage and conversion system: a mini review." *Catalysts* 10, no. 5 (2020): 495. https://doi.org/10.3390/catal10050495

[10] Huang, Kelei, Chunhu Li, Liang Wang, Wentai Wang, and Xiangchao Meng. "Layered Ti_3C_2 MXene and silver co-modified g-C_3N_4 with enhanced visible light-driven photocatalytic activity." *Chemical Engineering Journal* 425 (2021): 131493. https://doi.org/10.1016/j.cej.2021.131493

[11] Alhabeb, Mohamed, Kathleen Maleski, Babak Anasori, Pavel Lelyukh, Leah Clark, Saleesha Sin, and Yury Gogotsi. "Guidelines for synthesis and processing of two-dimensional titanium carbide (Ti_3C_2T x MXene)." *Chemistry of Materials* 29, no. 18 (2017): 7633-7644. https://doi.org/10.1021/acs.chemmater.7b02847

[12] Liu, Ning, Na Lu, Yan Su, Pu Wang, and Xie Quan. "Fabrication of g-C_3N_4/Ti_3C_2 composite and its visible-light photocatalytic capability for ciprofloxacin degradation." *Separation and Purification Technology* 211 (2019): 782-789. https://doi.org/10.1016/j.seppur.2018.10.027

[13] Peng, Chao, Xianfeng Yang, Yuhang Li, Hao Yu, Hongjuan Wang, and Feng Peng. "Hybrids of two-dimensional Ti_3C_2 and TiO_2 exposing {001} facets toward enhanced photocatalytic activity." *ACS Applied Materials & Interfaces* 8, no. 9 (2016): 6051-6060. https://doi.org/10.1021/acsami.5b11973

[14] Alsafari, Ibrahim A. "Synthesis of CuO/MXene nanocomposite to study its photocatalytic and antibacterial properties." *Ceramics International* 48, no. 8 (2022): 10960-10968. https://doi.org/10.1016/j.ceramint.2021.12.315

[15] Qu, Jie, Daoguang Teng, Xiaoman Zhang, Qianqian Yang, Peng Li, and Yijun Cao. "Preparation and regulation of two-dimensional Ti_3C_2Tx MXene for enhanced adsorption-photocatalytic degradation of organic dyes in wastewater." *Ceramics International* 48, no. 10 (2022): 14451-14459. https://doi.org/10.1016/j.ceramint.2022.01.338

[16] Saafie, N., M. F. R. Samsudin, S. Sufian, and R. M. Ramli. "Enhancement of the activated carbon over methylene blue removal efficiency via alkali-acid treatment." In *AIP Conference Proceedings*, vol. 2124, no. 1. AIP Publishing, 2019. https://doi.org/10.1063/1.5117106

[17] Liu, Wenzhu, Mingxuan Sun, Zhipeng Ding, Bowen Gao, and Wen Ding. "Ti_3C_2 MXene embellished g-C3N4 nanosheets for improving photocatalytic redox capacity." *Journal of Alloys and Compounds* 877 (2021): 160223. https://doi.org/10.1016/j.jallcom.2021.160223

[18] Im, Jong Kwon, Erica Jungmin Sohn, Sewoon Kim, Min Jang, Ahjeong Son, Kyung-Duk Zoh, and Yeomin Yoon. "Review of MXene-based nanocomposites for photocatalysis." *Chemosphere* 270 (2021): 129478. https://doi.org/10.1016/j.chemosphere.2020.129478

[19] Sun, Xiaoli, Baitao Zhang, Bingzheng Yan, Guoru Li, Hongkun Nie, Kejian Yang, Chengqian Zhang, and Jingliang He. "Few-layer Ti_3C_2T x (T= O, OH, or F) saturable absorber for a femtosecond bulk laser." *Optics Letters* 43, no. 16 (2018): 3862-3865. https://doi.org/10.1364/OL.43.003862

[20] Jaffari, Zeeshan Haider, Salahaldin M. A. Abuabdou, Ding-Quan Ng, and Mohammed J. K. Bashir. "Insight into two-dimensional MXenes for environmental applications: Recent progress, challenges, and prospects." *FlatChem* 28 (2021): 100256. https://doi.org/10.1016/j.flatc.2021.100256

[21] Long, Runxuan, Zongxue Yu, Qiuyue Tan, Xiaofang Feng, Ximei Zhu, Xuyang Li, and Pingquan Wang. "Ti_3C_2 MXene/NH_2-MIL-88B (Fe): Research on the adsorption kinetics and photocatalytic performance of an efficient integrated photocatalytic adsorbent." *Applied Surface Science* 570 (2021): 151244. https://doi.org/10.1016/j.apsusc.2021.151244